

Strain accumulation in sand due to drained cyclic loading: on the effect of monotonic and cyclic preloading (Miner's rule)

T. Wichtmannⁱ⁾, A. Niemunisⁱⁱ⁾, Th. Triantafyllidisⁱⁱⁱ⁾

Abstract:

An experimental validation of Miner's rule for freshly pluviated sand is presented. Drained triaxial tests with four packages of 25,000 cycles applied in different sequences have been performed. It is demonstrated that an effect of the sequence of application on the "cyclic flow rule" $\dot{\varepsilon}_q^{\text{acc}}/\dot{\varepsilon}_v^{\text{acc}}$ and on the final value of the residual strain ε^{acc} can be neglected for practical purposes. In contrast to the significant reduction in the rate of accumulation caused by a cyclic preloading, only a slight decrease of the intensity of accumulation $\dot{\varepsilon}^{\text{acc}}$ was measured after a drained monotonic preloading. The cyclic flow rule remains unchanged by the monotonic preloading. These experimental findings are considered in the high-cycle accumulation (HCA) model proposed by the authors. Re-calculations of the laboratory tests with the HCA model confirm a good prediction. A change of $\dot{\varepsilon}_q^{\text{acc}}/\dot{\varepsilon}_v^{\text{acc}}$ and $\dot{\varepsilon}^{\text{acc}}$ due to changes of the average stress σ^{av} needs further investigations.

Keywords: sand, drained cyclic triaxial tests, accumulation of strain, monotonic preloading, cyclic preloading, Miner's rule, high-cycle accumulation model

1 Introduction

The high-cycle accumulation (HCA) model proposed by the authors [8] predicts permanent settlements or excess pore water pressures due to a high-cyclic loading, that means a large number of cycles ($N > 10^3$) with small strain amplitudes ($\varepsilon^{\text{ampl}} < 10^{-3}$). The basic constitutive equation of the model reads

$$\dot{\sigma} = \mathbf{E} : (\dot{\varepsilon} - \dot{\varepsilon}^{\text{acc}} - \dot{\varepsilon}^{\text{pl}}) \quad (1)$$

with the rate $\dot{\sigma}$ of the effective stress σ , the elastic stiffness \mathbf{E} , the strain rate $\dot{\varepsilon}$, the prescribed strain accumulation rate $\dot{\varepsilon}^{\text{acc}}$ and the plastic strain rate $\dot{\varepsilon}^{\text{pl}}$. The superposed dot means a derivative with respect to the number of cycles, i.e. $\dot{\square} = \partial \square / \partial N$. The strain accumulation rate is calculated as the product $\dot{\varepsilon}^{\text{acc}} = \dot{\varepsilon}^{\text{acc}} \mathbf{m}$ of the scalar *intensity* of strain accumulation $\dot{\varepsilon}^{\text{acc}} = \|\dot{\varepsilon}^{\text{acc}}\|$ and the tensorial *direction* of strain accumulation $\mathbf{m} = \dot{\varepsilon}^{\text{acc}} / \|\dot{\varepsilon}^{\text{acc}}\|$ (unit tensor). In the axisymmetric triaxial case the intensity of accumulation is $\dot{\varepsilon}^{\text{acc}} = \sqrt{(\dot{\varepsilon}_1^{\text{acc}})^2 + 2(\dot{\varepsilon}_3^{\text{acc}})^2}$ with ε_1 and $\varepsilon_2 = \varepsilon_3$ being the axial and lateral strain components, respectively. The direction of strain accumulation is fully described by the ratio $\dot{\varepsilon}_q^{\text{acc}}/\dot{\varepsilon}_v^{\text{acc}}$ with the deviatoric strain rate $\dot{\varepsilon}_q = 2/3(\dot{\varepsilon}_1 - \dot{\varepsilon}_3)$ and the volumetric strain rate $\dot{\varepsilon}_v = \dot{\varepsilon}_1 + 2\dot{\varepsilon}_3$.

The HCA model considers that the direction of strain accumulation $\dot{\varepsilon}_q^{\text{acc}}/\dot{\varepsilon}_v^{\text{acc}}$ depends only on the average stress ratio $\eta^{\text{av}} = q^{\text{av}}/p^{\text{av}}$ with p and q being Roscoe's invariants. In the triaxial case $p = (\sigma_1 + 2\sigma_3)/3$ and $q = \sigma_1 - \sigma_3$ hold with σ_1 and $\sigma_2 = \sigma_3$ being the axial and lateral stress components, respectively. The intensity of strain accumulation $\dot{\varepsilon}^{\text{acc}}$ is a function of strain amplitude, void ratio, average stress and cyclic preloading. Results of numerous drained cyclic triaxial and multiaxial direct simple shear

tests [14–16] served as a basis for the HCA model. Details of the model are discussed in [8].

The HCA model takes packages of constant-amplitude cycles as input. A loading with varying amplitudes (e.g. traffic loading, wind and wave loading) must be decomposed into such packages (Fig. 1). The procedure is based on the assumption, that the sequence of the packages is of minor importance for the final residual deformation, that means that Miner's rule [7] known from fatigue mechanics of metals is applicable to sand. The present paper provides the experimental evidence. Triaxial tests on sand with four packages of 25,000 cycles each applied in different sequences are presented (Section 4). The measured accumulation rates are fairly well predicted by the HCA model.

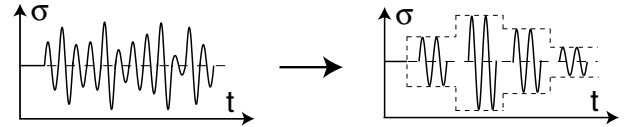


Fig. 1: A loading with varying amplitudes is decomposed into packages each with a constant amplitude

At present the HCA model does not consider a monotonic preloading history as an influencing parameter. A monotonic preloading is understood here as the single application of a stress which is much larger than the average stress during the subsequent cycles. The present paper provides evidence that the effect of such preloading up to an effective mean pressure $p = 300$ kPa can be neglected for practical purpose. In the drained cyclic triaxial tests, $N = 10^4$ cycles have been applied after a drained monotonic preloading along an isotropic or K_0 -stress path, respectively. To the authors' best knowledge, such experiments have not been documented in the literature yet.

If the average stress σ^{av} is changed between two packages of cycles, the flow rule $\dot{\varepsilon}_q^{\text{acc}}/\dot{\varepsilon}_v^{\text{acc}}$ and the intensity of accumulation $\dot{\varepsilon}^{\text{acc}}$ in the later package may significantly differ from the values observed for freshly pluviated sand at

ⁱ⁾Research Assistant, Institute of Soil Mechanics and Rock Mechanics, University of Karlsruhe, Germany (corresponding author). Email: torsten.wichtmann@ibf.uka.de

ⁱⁱ⁾Research Assistant, Institute of Soil Mechanics and Rock Mechanics, University of Karlsruhe, Germany

ⁱⁱⁱ⁾Professor and Director of the Institute of Soil Mechanics and Rock Mechanics, University of Karlsruhe, Germany

same σ^{av} (Section 6). The effect of such combined monotonic and cyclic preloading needs further investigation and may necessitate an extension of the HCA model.

2 Literature review

Miner's rule [7] has been developed in order to estimate the fatigue of metals subjected to a cyclic loading with varying amplitudes. If N_{fi} is the number of cycles to failure for a constant amplitude σ_i^{ampl} , the failure criterion for varying amplitudes can be expressed as

$$\sum_{i=1}^n \frac{N_i}{N_{fi}} = 1, \quad (2)$$

wherein N_i is the number of cycles applied with the amplitude σ_i^{ampl} . Accordingly, the sequence of the amplitudes is irrelevant.

For a low number of cycles ($N < 150$) Miner's rule has been experimentally confirmed for a calcareous sand by Kaggwa et al. [6]. Kaggwa et al. performed triaxial tests with a constant average stress and with three packages of 50 cycles applied with amplitudes $q^{\text{ampl}} = 100, 150$ and 200 kPa. Their sequence hardly influenced the final values of the residual volumetric and shear strain, Fig. 2 ($\gamma = \varepsilon_1 - \varepsilon_3$).

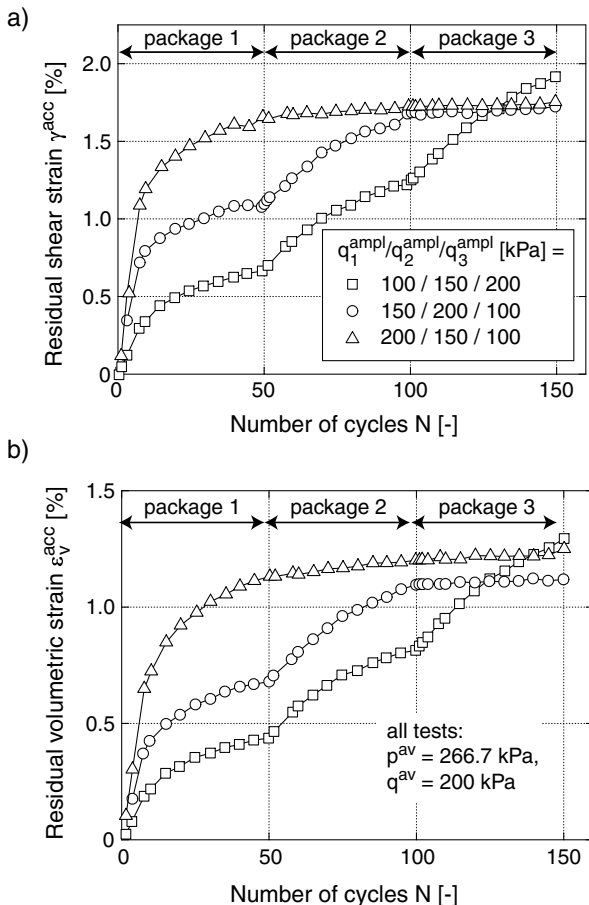


Fig. 2: Residual a) shear and b) volumetric strains in tests with packages of cycles performed by Kaggwa et al. [6]

Some research on the effect of a cyclic loading with varying amplitudes has been done in the field of geotechnical earthquake engineering. Random cyclic loading histories

were tested under undrained conditions for example by Ishihara & Yasuda [4, 5], Ishihara & Nagase [2] and Tatsuoka et al. [13]. In order to estimate the risk of liquefaction, a random cyclic loading is usually replaced by an equivalent number of cycles with a constant amplitude (e.g. Seed & Idriss [9], Seed et al. [10]). "Equivalent" means the same build-up of excess pore water pressure after all cycles have been applied. The constant amplitude is chosen as a certain fraction (e.g. 65 %) of the maximum amplitude of the random cyclic loading.

The influence of a monotonic preloading on strain or pore pressure accumulation was rarely studied in the literature. Some undrained cyclic tests on specimens preloaded monotonically towards different *OCR*-values (Ishihara & Takatsu [3], Seed & Peacock [11]) showed an increase of the liquefaction resistance with increasing *OCR*. A significant change of the undrained *monotonic* shear behaviour due to a monotonic preloading has been experimentally found by Doanh et al. [1] for extremely loose specimens prepared by moist tamping.

3 Tested material and testing procedure

All tests were performed on a poorly graded medium coarse quartz sand with a subangular grain shape. It has a mean grain size of $d_{50} = 0.55$ mm and a coefficient of uniformity $C_u = d_{60}/d_{10} = 1.8$. The grain size distribution curve is given in Fig. 4 of [14] (denoted as Sand No. 1).

A scheme of the cyclic triaxial device used for the present study has also been shown by Wichtmann et al. [14]. Cylindrical specimens (diameter $d = 10$ cm, height $h = 20$ cm) were prepared using the air pluviation technique. After flushing with CO_2 , they were saturated with de-aired water. Using a back pressure of 200 kPa Skempton's *B*-value was > 0.98 in all tests. The cell pressure was kept constant in the tests of the present study. The axial load was applied with a pneumatic loading system and was measured inside the pressure cell below the specimen base. Axial deformations were measured with a displacement transducer attached to the load piston. The system compliance known from preliminary tests with a steel dummy was subtracted. Volume changes were determined via the pore water using a burette system and a differential pressure transducer.

First the average stress σ^{av} was applied and maintained for a period of one hour. Next, the cyclic loading was commenced. Some of the cyclic tests were preceded by a monotonic preloading (Section 5) while some were not. The first *irregular* cycle of each package was applied at a low frequency $f = 0.01$ Hz. The subsequent *regular* cycles were applied at a frequency of 0.25 Hz in the tests on Miner's rule and at 0.1 Hz in the tests with a monotonic preloading. In accordance with the literature (see e.g. [12, 20]) Wichtmann et al. [14] have demonstrated that the loading frequency does not affect the accumulation of residual strain in the tested range $0.05 \text{ Hz} \leq f \leq 2 \text{ Hz}$.

4 Validation of Miner's rule

Six tests were performed with the same average stress ($p^{\text{av}} = 200$ kPa, $\eta^{\text{av}} = q^{\text{av}}/p^{\text{av}} = 0.75$) and with initially medium dense specimens ($0.58 \leq I_{D0} \leq 0.63$). Four packages, each with 25,000 cycles, were applied in succession. The deviatoric stress amplitudes $q^{\text{ampl}} = 20, 40, 60$ and 80 kPa were tested in different sequences (see a scheme in Figure 3).

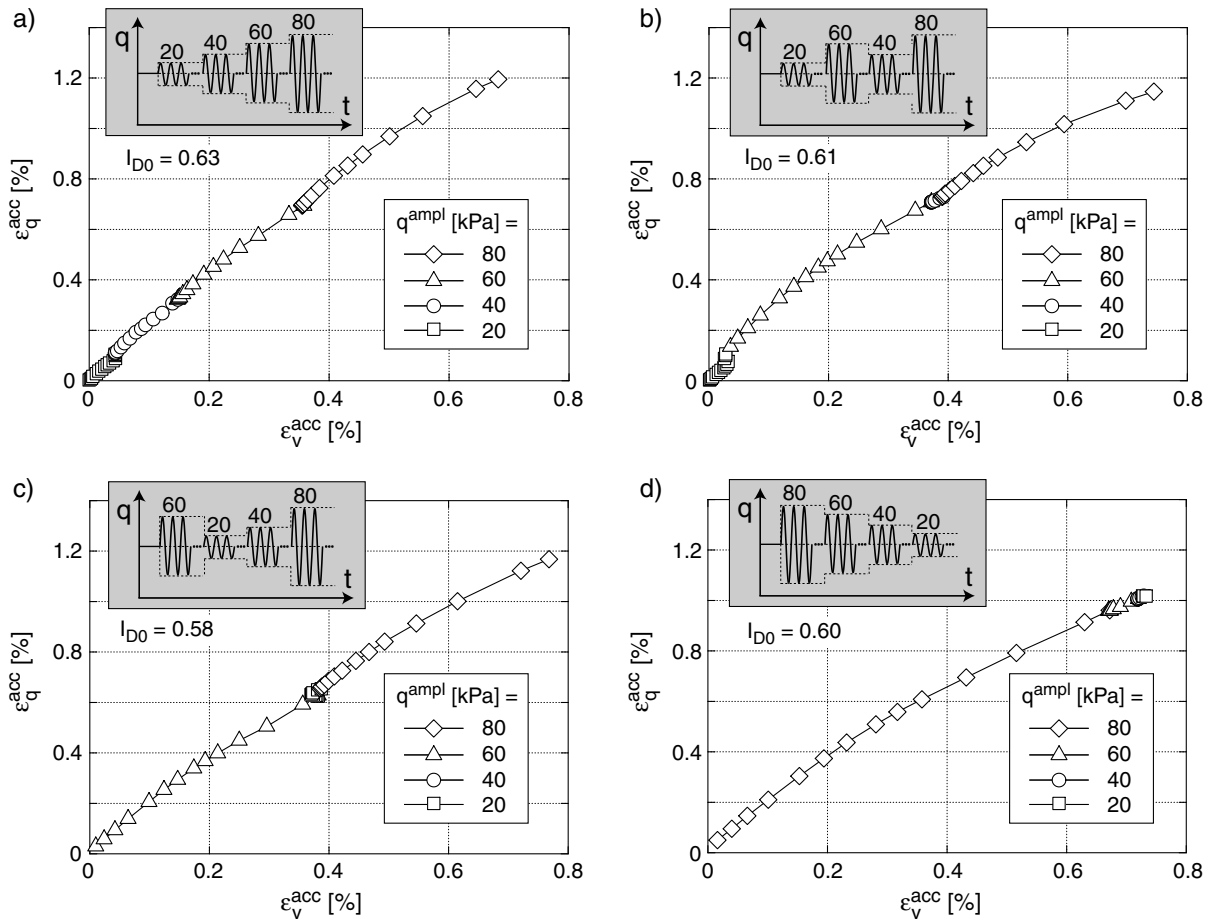


Fig. 4: ε_q^{acc} - ε_v^{acc} -strain paths in four tests with amplitudes $q^{ampl} = 20, 40, 60$ and 80 kPa applied in different sequences ($p^{av} = 200$ kPa, $\eta^{av} = 0.75$, $f = 0.25$ Hz)

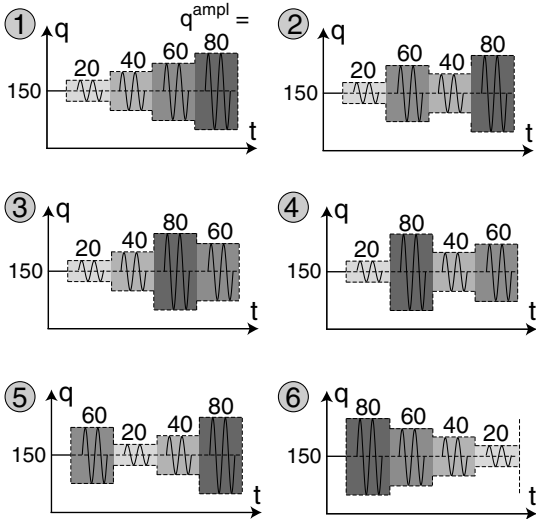


Fig. 3: Tested sequences of the amplitudes $q^{ampl} = 20, 40, 60$ and 80 kPa

Fig. 4 shows that the effect of the sequence of application of the packages on the "cyclic flow rule" $\dot{\varepsilon}_q^{acc}/\dot{\varepsilon}_v^{acc}$ is negligible. The direction of the strain paths in the ε_q^{acc} - ε_v^{acc} -diagram hardly changes due to a change in the amplitude. At the most, a small increase of the ratio $\dot{\varepsilon}_q^{acc}/\dot{\varepsilon}_v^{acc}$ was

measured at the beginning of a package if q^{ampl} was increased and if no larger stress amplitude had been applied previously.

The diagrams showing q versus ε_1 in Figure 5 demonstrate that the residual strain in the first, irregular cycle of each package depends on the sequence of application. Considering the test $20 \rightarrow 80 \rightarrow 40 \rightarrow 60$ (Fig. 5d), the package with small cycles (here $q^{ampl} = 20$ kPa) affects the stiffness during the first, irregular cycle of the subsequent package with a larger amplitude (here $q^{ampl} = 80$ kPa). During the initial phase of the irregular cycle the stiffness is similar to the secant stiffness of the previous small cycles (here until a deviatoric stress $q \approx q^{av} + 3q^{ampl} = 210$ kPa is reached). Therefore, the residual strain due to this irregular cycle is significantly reduced, compared to a test in which the same amplitude is applied in the first package (Fig. 5f). The residual strains due to the first cycles of each package are extremely small for a sequence $20 \rightarrow 40 \rightarrow 60 \rightarrow 80$ (Figure 5a). The earlier the packages with large amplitudes are applied, the larger are the residual deformations in their first cycles.

Figure 6a shows the accumulation curves $\varepsilon^{acc}(N)$ including the residual strain due to the first cycles of each package. The residual strain ε^{acc} at the end of the fourth package was the larger, the earlier the packages with the large amplitudes $q^{ampl} \geq 60$ kPa were applied. This can be attributed to the larger residual strains in the first cycles (Figure 5). If one subtracts the strains accumulated in the

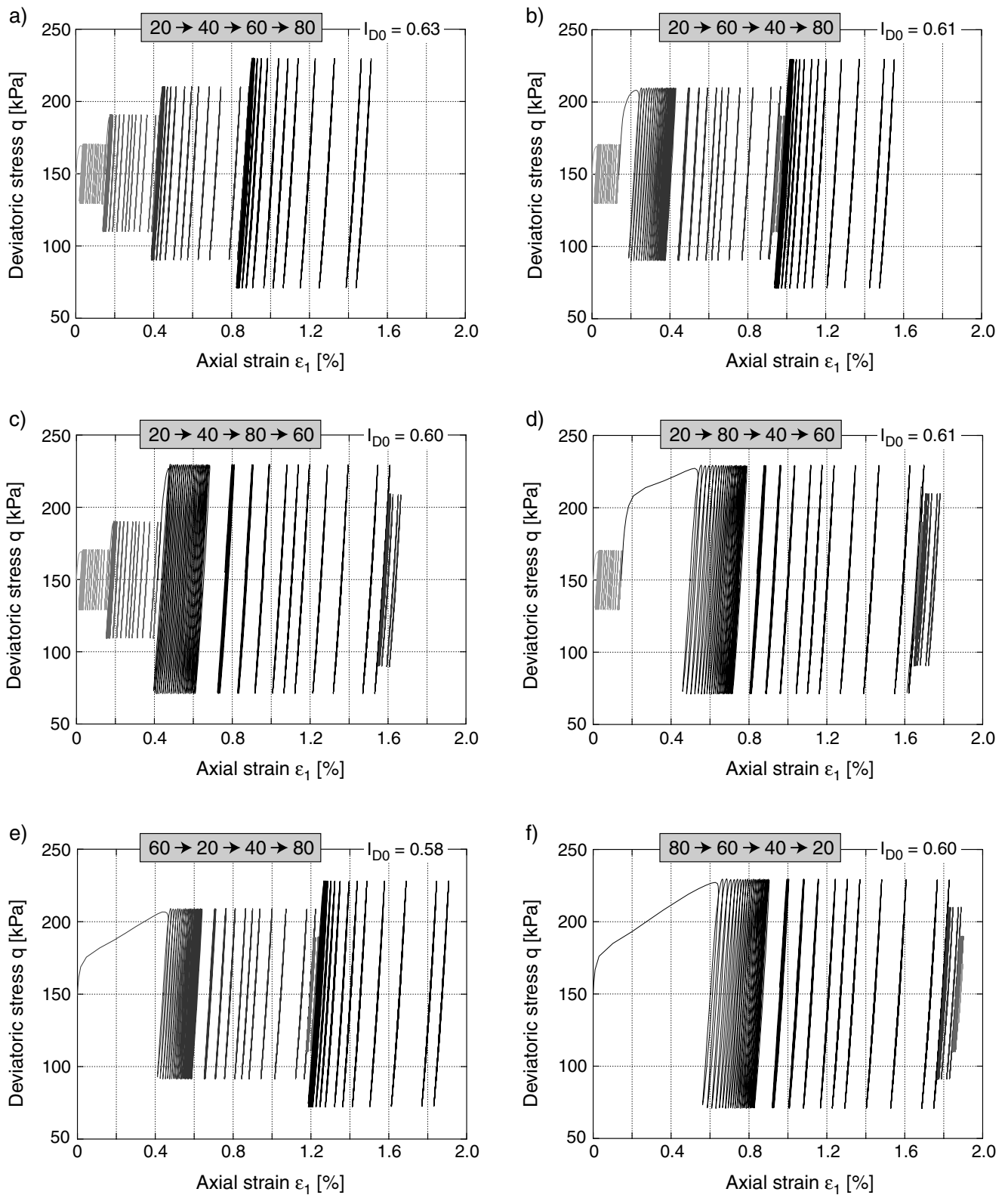


Fig. 5: q - ϵ_1 -diagrams in six tests with packages of cycles with amplitudes $q^{ampl} = 20, 40, 60$ and 80 kPa applied in different sequences. The diagrams show the first 25 cycles and 5 cycles at $N = 50, 100, 200, 500, 1000, 2000, 5000, 10000, 20000$ and 25000 .

first cycles of each package (Figure 6b) the residual strain at the end of a test is the larger the later the packages with the large amplitudes are applied. The slower accumulation during the regular cycles in the tests with an early application of the large amplitudes can be explained with the larger compaction in the first cycles. The smaller void ratios cause smaller accumulation rates.

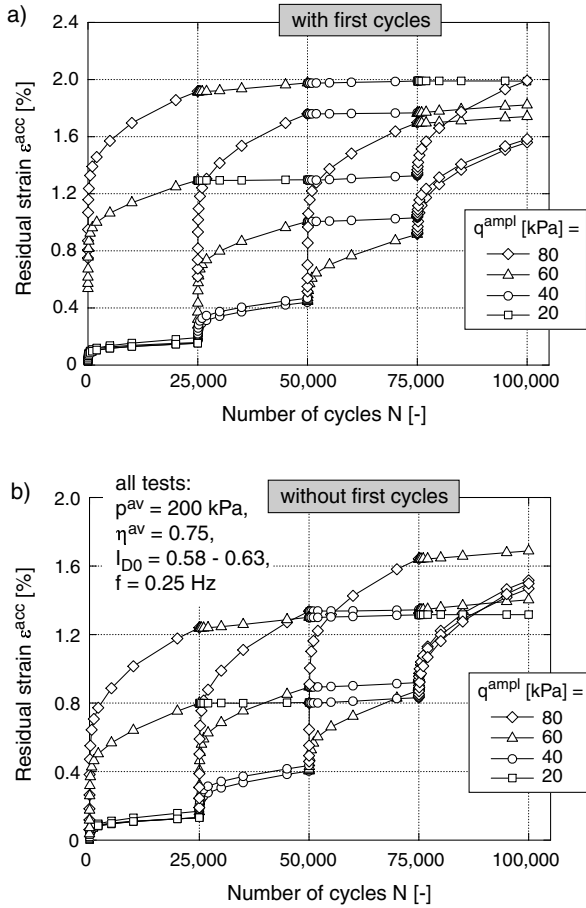


Fig. 6: Accumulation curves $\varepsilon^{acc}(N)$: a) with and b) without the residual strains in the first cycles

From Figure 6 it may be concluded, that the influence of the sequence of application of packages of cycles on the final value of the residual strain is only moderate. Therefore, it seems justified to neglect the influence of the sequence of application in a HCA model.

The validity of Miner's rule seems to be independent of the number of applied cycles, since it was confirmed for 100 cycles per package by Kaggwa et al. [6] and for 25,000 cycles per package by the present test series. However, for very large numbers of cycles $N > 10^5$ per package Miner's rule has not been confirmed yet. It is likely that the results of the present test series would be similar for a wide range of clean sands, since the basic characteristics of strain accumulation were found similar for several quartz sands with different grain size distribution curves [17, 18]. Since the initial fabric, that means the method of sample preparation has been found to influence both, the intensity of accumulation and the cyclic flow rule [19], it may also affect Miner's rule. Up to now, Miner's rule has been validated only for air-pluviated sand samples of medium density. Furthermore, Miner's rule has been confirmed only for

the case of an uniaxial cyclic loading. If the polarization, that means the direction of the cycles changes between subsequent packages, the sequence of application may not be irrelevant anymore. The effect of moisture content on the various components of the HCA model, amongst them on the validity of Miner's rule is also unclear so far. All these open questions need further experimental investigations in the future.

Finally, the test results are briefly discussed regarding the elastic portion of strain. For larger stress amplitudes $q^{ampl} \geq 60$ kPa a considerable decrease of the strain amplitude ε^{ampl} with N is usually observed during the first 100 cycles [14] (so-called "conditioning phase"). In the present tests such decrease could be observed only, if no larger amplitude q^{ampl} was applied previously. This becomes clear from Figure 7 which shows the development of the strain amplitude with N in the two tests with the sequences $20 \rightarrow 40 \rightarrow 60 \rightarrow 80$ and $80 \rightarrow 60 \rightarrow 40 \rightarrow 20$.

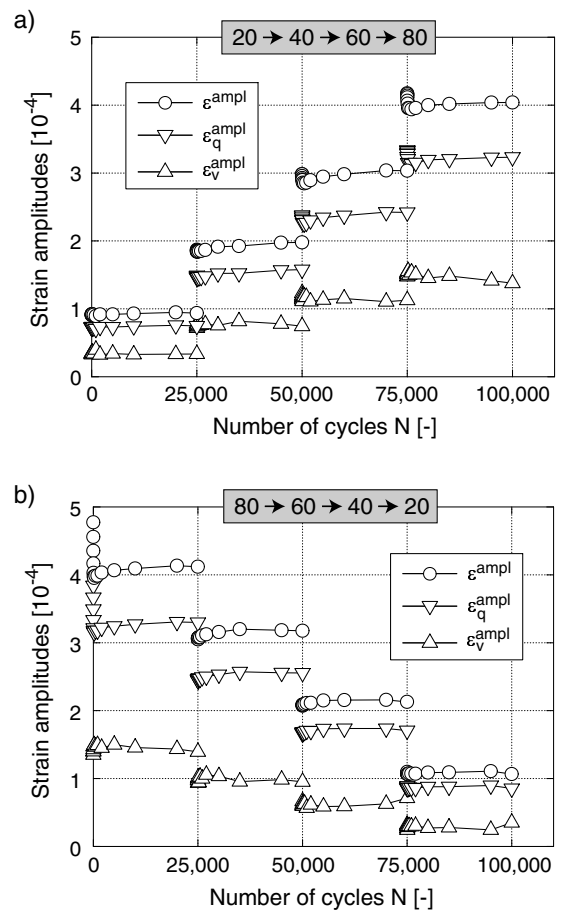


Fig. 7: Strain amplitudes ε^{ampl} , ε_v^{ampl} and ε_q^{ampl} as a function of the number of cycles N in two of the tests

The HCA model proposed by Niemunis et al. [8] obeys Miner's rule due to its historiotropic variable g^A . It quantifies the cyclic preloading containing an information about the number N of previous cycles and about their strain amplitude ε^{ampl} . The prediction of the HCA model for 10^5 cycles, half of them with $\varepsilon^{ampl} = 2 \cdot 10^{-4}$ and the other half with $\varepsilon^{ampl} = 4 \cdot 10^{-4}$, is shown in Fig. 8. Obviously, the residual strain does not depend on the number of packages or on their sequence.

The prediction of the HCA model for the six tests is

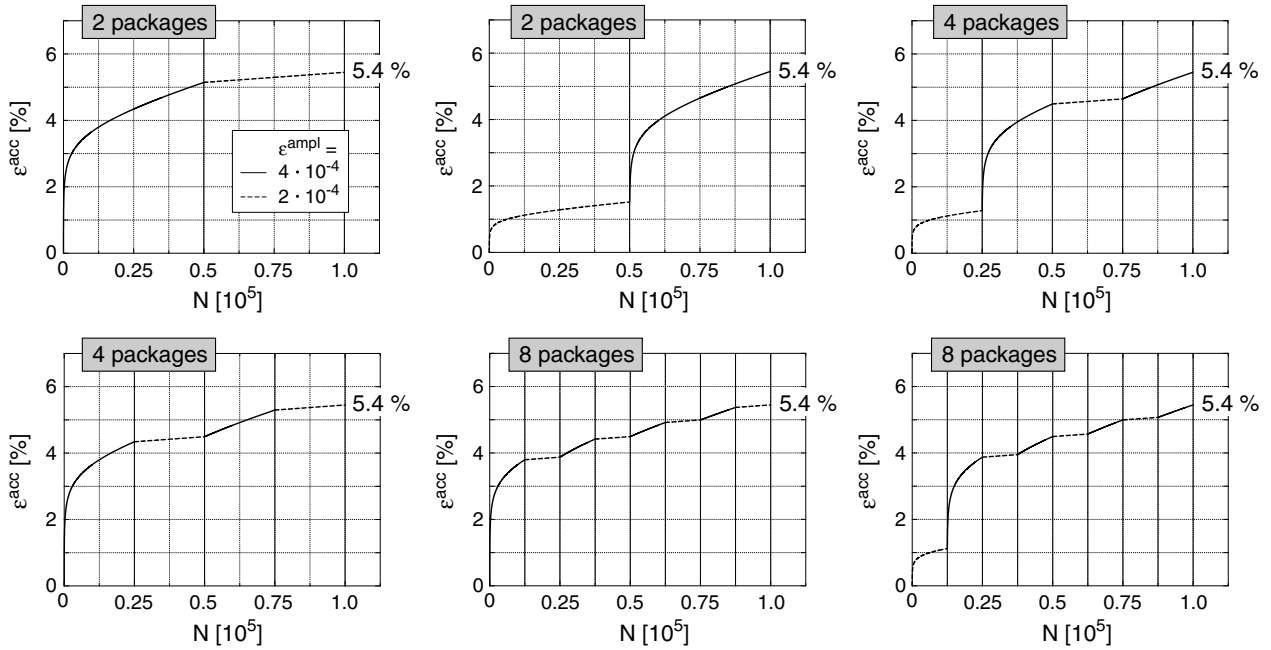


Fig. 8: Predicted accumulation curves $\varepsilon^{acc}(N)$ during 10^5 cycles with strain amplitudes $\varepsilon^{ampl} = 2 \cdot 10^{-4}$ or $\varepsilon^{ampl} = 4 \cdot 10^{-4}$, applied in different packages and sequences ($e = e_{max} = 0.874$, $p^{av} = 100$ kPa, $\eta^{av} = 0$, that means $f_e = f_p = f_Y = 1$, HCA model parameters taken from Table 1)

Parameter	Value
C_{ampl}	1.76
C_e	0.53
e_{ref}	0.874
C_p	0.42
C_Y	2.06
C_{N1}	$3.6 \cdot 10^{-4}$
C_{N2}	0.42
C_{N3}	$5.0 \cdot 10^{-4}$

Table 1: Parameters of the HCA model used for the recalculation of the element tests (C_{ampl} = exponent of function f_{ampl})

compared to the measured data in Figure 9. The material constants of the HCA model given in Table 1 and the measured strain amplitudes $\varepsilon^{ampl}(N)$ were used as input. The constants in Table 1 differ from those derived by Wichtmann et al. [14] since recent test results [18] have shown that the exponent C_{ampl} of the amplitude function $f_{ampl} = (\varepsilon^{ampl}/10^{-4})^{C_{ampl}}$ should be treated as an additional material constants rather than setting it to the constant value of 2.0. Therefore, the data provided by Wichtmann et al. [14] have been re-analyzed delivering the parameters collected in Table 1. Despite some deviations between the experimental and the recalculated data, the HCA model reproduces well the change of the accumulation rate due to a change of the amplitude, considering the prior cyclic loading (Figure 9).

5 Influence of a monotonic preloading

Starting from $p = 50$ kPa, medium dense specimens were monotonically preloaded up to a mean pressure of $p_{preload} = 200$ or 300 kPa, respectively, either along the isotropic axis ($\eta = q/p = 0$) or along a K_0 -stress path ($\eta = 0.75$), Figure

10. These preloading pressures are well below values for which significant particle breakage would be expected. The preloading pressure was maintained over a period of five minutes. Next, the specimens were unloaded to $p = 100$ kPa along the same stress path. Subsequently, 10^4 cycles with a stress amplitude $q^{ampl} = 50$ kPa were applied at $p^{av} = 100$ kPa and $\eta^{av} = 0$ or 0.75 , respectively. Additional tests on specimens without a preloading (denoted by $p_{preload} = 100$ kPa in the following diagrams) have also been performed for comparison purposes.

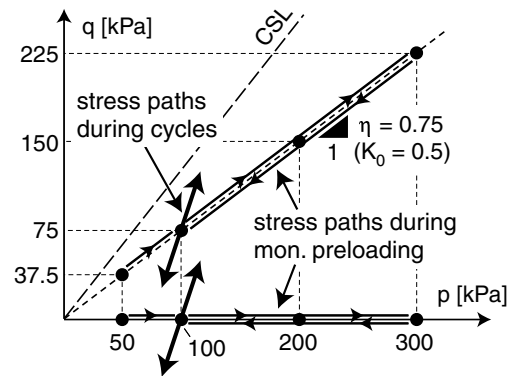


Fig. 10: Stress paths in the tests with monotonic preloading

The "cyclic flow rule" is not influenced by the monotonic preloading. This becomes clear from the $\varepsilon_q^{acc} - \varepsilon_v^{acc}$ -strain paths given in Figure 11. For both, a preloading along $\eta = 0$ and along $\eta = 0.75$, the directions of the strain paths coincide for different values of $p_{preload}$.

The accumulation curves $\varepsilon^{acc}(N)$ in the tests with $p_{preload} = 200$ kPa hardly differ from those obtained for the non-preloaded specimens. This applies for both, the preloading along $\eta = 0$ (Figure 12a) and along $\eta = 0.75$

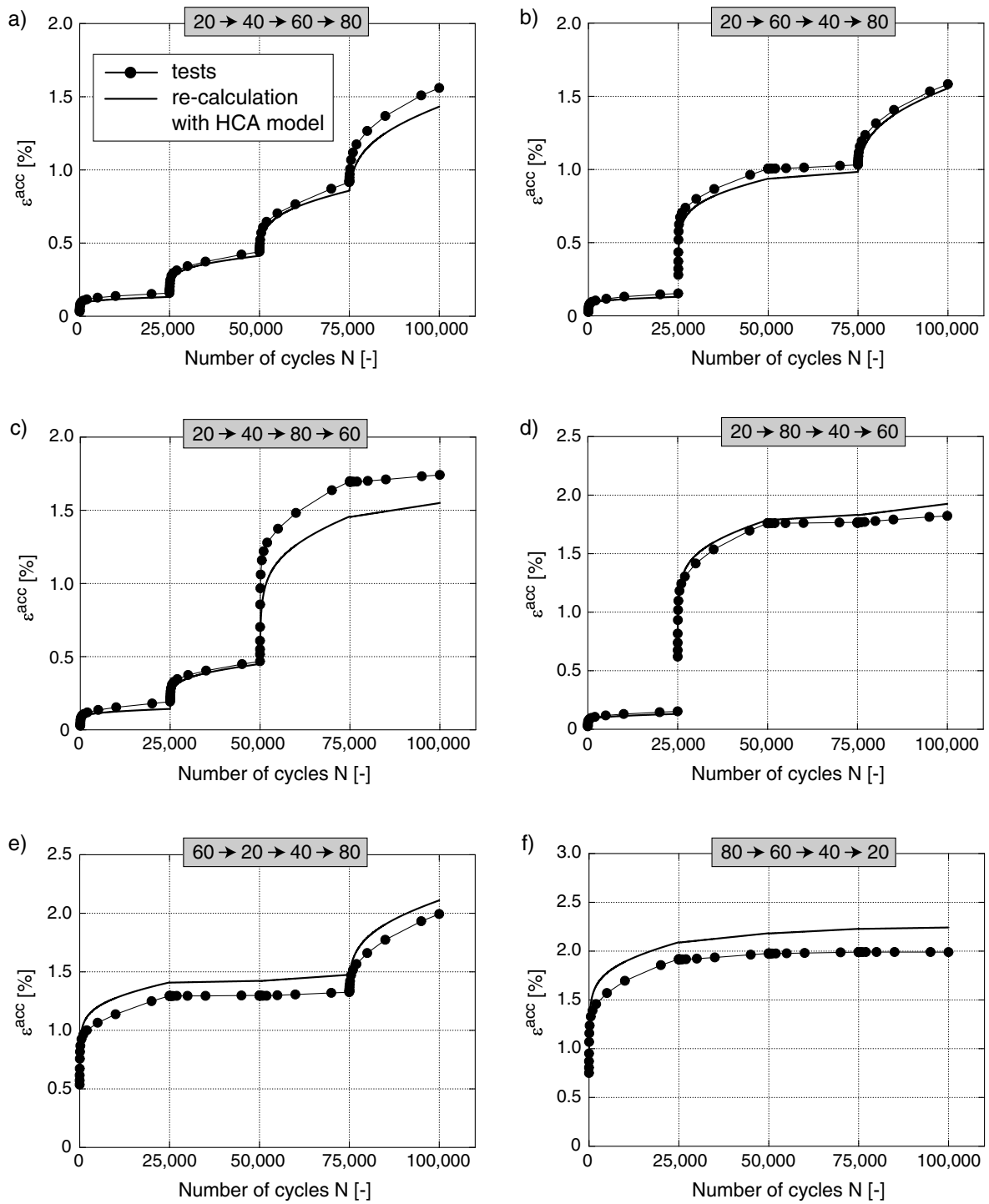


Fig. 9: Re-calculation of the six cyclic triaxial tests with packages of cycles using the HCA model and the parameters given in Table 1

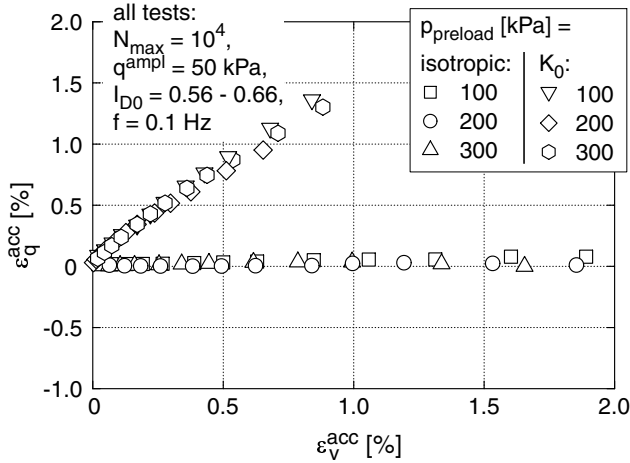


Fig. 11: $\epsilon_q^{\text{acc}} - \epsilon_v^{\text{acc}}$ -strain paths during 10^4 cycles applied after a monotonic preloading up to different preloading pressures p_{preload}

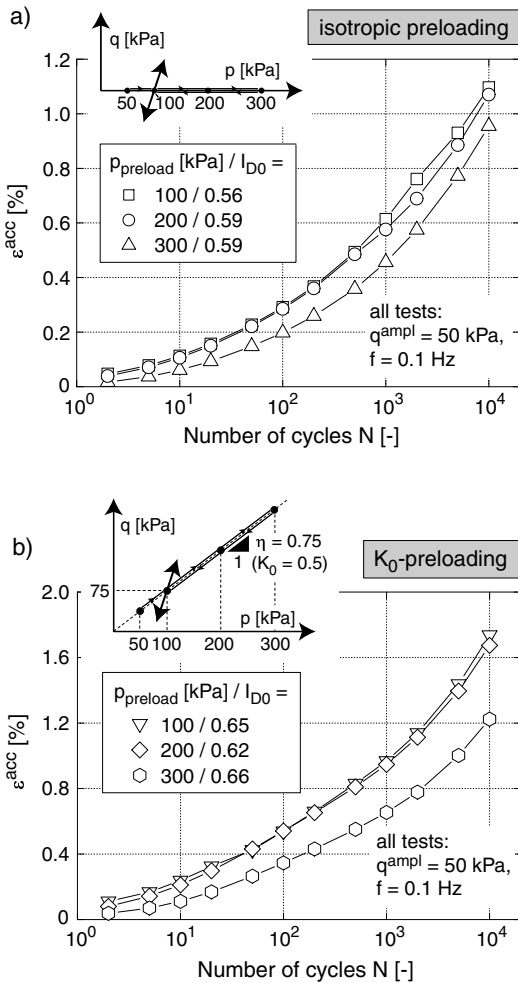


Fig. 12: Accumulation curves $\epsilon^{\text{acc}}(N)$ after a monotonic preloading applied a) along $\eta = 0$ and b) along $\eta = 0.75$

(Figure 12b). Despite a similar initial density I_{D0} the accumulation rates of the specimens preloaded up to $p_{\text{preload}} = 300$ kPa were slightly lower. This finding is in agreement with the results of Ishihara & Takatsu [3] or Seed & Peacock [11] concerning the rate of pore water pressure accumulation in undrained tests. It may be attributed to fabric changes during monotonic preloading which seem to become significant only for larger values of p_{preload} . The accumulation rate $\dot{\epsilon}^{\text{acc}}$ is much less affected by a monotonic preloading than by a cyclic one, at least for specimens prepared by air pluviation. Therefore, it is justified to neglect the effect of a monotonic preloading in the HCA model.

The experiments of Doanh [1] indicate, however, that the influence of a monotonic preloading may be more pronounced for very loose specimens prepared by moist tamping. Therefore, the initial density and the method of sample preparation (initial fabric) may affect the change of the intensity of accumulation $\dot{\epsilon}^{\text{acc}}$ or the flow rule $\dot{\epsilon}_q^{\text{acc}} / \dot{\epsilon}_v^{\text{acc}}$ due to a monotonic preloading. Furthermore, the effect of a monotonic preloading could be more pronounced if both, the preloading and the subsequent cycles have the same polarization, for example if the isotropic preloading is followed by cycles along the p -axis. Further research on the influence of a monotonic preloading under such conditions is necessary.

6 Effect of a change of the average stress

A combination of a monotonic and a cyclic preloading was also tested in a drained triaxial test on a medium dense specimen. Packages of 100 cycles were applied at different average stresses σ^{av} in succession. The amplitude-pressure ratio $q^{\text{ampl}} / p^{\text{av}} = 0.3$ was the same for all packages. The average stress was $p^{\text{av}} = 200$ kPa, $\eta^{\text{av}} = 0.75$ in the packages Nos. 1,3,5 and 7 (see a scheme in Figure 13). In package No. 2 the average stress ratio was increased to $\eta^{\text{av}} = 1.1$. In the packages Nos. 4 and 6 the average mean pressure was decreased to $p^{\text{av}} = 100$ kPa or increased to $p^{\text{av}} = 300$ kPa, respectively.

In Figure 14 the cyclic flow rule is shown as a unit vector with origin at the average stress σ^{av} of the respective package of cycles and inclined accordingly to the measured ratio $\dot{\epsilon}_q^{\text{acc}} / \dot{\epsilon}_v^{\text{acc}}$ of the strain accumulation rates. During the first two packages of cycles, the "cyclic flow rule" agreed well with the flow rule of the Modified Cam-Clay (MCC) model (Figure 14a,b, see also [14]). However, the cyclic preloading at $\eta^{\text{av}} = 1.1$ drastically changed the flow rule towards a more isotropic accumulation in the subsequent packages at smaller average stress ratios (Figure 14c-f). During the packages Nos. 3 and 4 even a negative rate of deviatoric strain accumulation $\dot{\epsilon}_q^{\text{acc}} < 0$ was measured. With increasing number of cycles, a slight rotation of the vectors back towards the MCC flow rule was observed. The difference to the MCC flow rule became less pronounced in package No. 6 applied at $p^{\text{av}} = 300$ kPa, probably because of a smaller distance to the preloading surface.

The comparison of the accumulation rates $\dot{\epsilon}^{\text{acc}}$ (Figure 15b) in the packages with $p^{\text{av}} = 200$ kPa and $\eta^{\text{av}} = 0.75$ (Nos. 1,3,5 and 7) with a reference test at constant σ^{av} reveals that a change of σ^{av} temporarily increases the intensity of accumulation $\dot{\epsilon}^{\text{acc}}$. A similar effect is observed if the polarization of the cycles is suddenly changed [15]. The decrease of the rate $\dot{\epsilon}^{\text{acc}}$ after a change of σ^{av} is faster than in the reference test at the same N -value.

Therefore, if a cyclic loading is preceded by a cyclic preloading at a considerably different average stress, then both the cyclic flow rule and the expression for the intensity of accumulation proposed in the HCA model become inaccurate. For a description of this effect in the HCA model further experimental investigations are necessary.

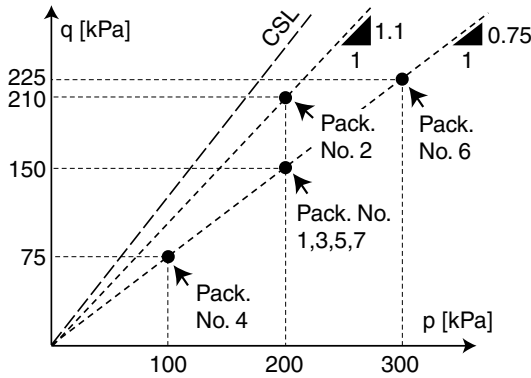


Fig. 13: Subsequent application of packages with 100 cycles at different average stresses σ^{av}

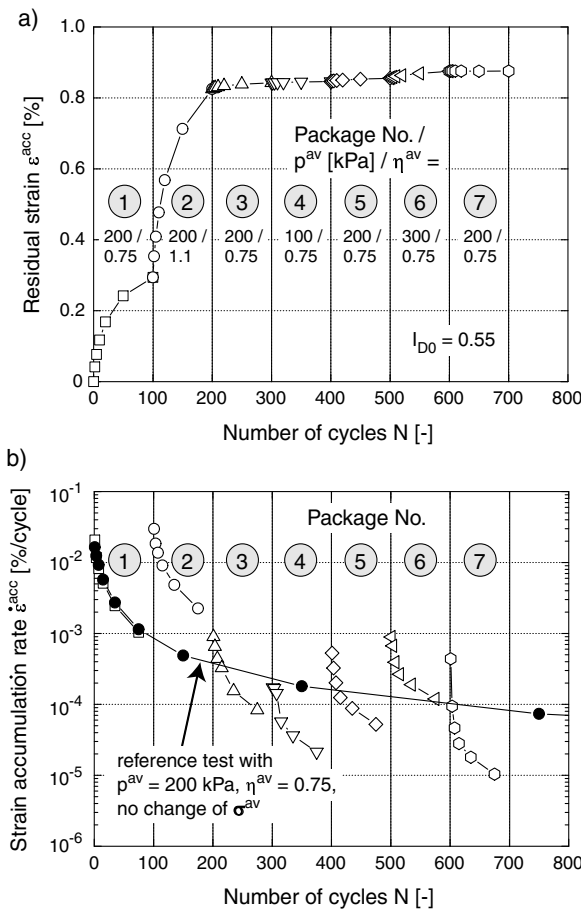


Fig. 15: a) Accumulation curve $\varepsilon^{acc}(N)$ (without the first cycle of each package) and b) rates $\dot{\varepsilon}^{acc} \approx \Delta\varepsilon^{acc}/\Delta N$ in tests with a change of the average stress σ^{av} between packages of cycles

7 Summary, conclusions and outlook

The validity of Miner’s rule has been confirmed for freshly pluviated sand of medium density in drained triaxial tests with an uniaxial cyclic loading. Four packages of 25,000 cycles with different amplitudes have been applied in different sequences. The direction of accumulation (cyclic flow rule) turned out to be hardly influenced by the sequence of the packages. The final values of the residual strain were also similar (20 % differences at most). The HCA model proposed by the authors [8] obeys Miner’s rule and predicts fairly well the measured curves $\varepsilon^{acc}(N)$. However, further research is necessary particularly with regard to the validity of Miner’s rule for a change of the polarization between subsequent packages of cycles and for sample preparation methods others than air pluviation (different initial fabric).

A monotonic preloading does not affect the cyclic flow rule $\dot{\varepsilon}_q^{acc}/\dot{\varepsilon}_v^{acc}$ and decreases only moderately the intensity of accumulation $\dot{\varepsilon}^{acc}$ for freshly pluviated sand of medium density, at least in the range of tested preloading pressures $p_{preload} \leq 300$ kPa. This applies to both, an isotropic and a K_0 -preloading. Consistently, the effect of a monotonic preloading has been neglected in the HCA model. However, a larger effect may be observed for very low initial densities, for sample preparation methods others than air pluviation or for cycles applied with the same polarization as the preloading. This should be clarified in further experiments in the future.

A significant change of the average stress σ^{av} between two packages of cycles strongly changes the cyclic flow rule $\dot{\varepsilon}_q^{acc}/\dot{\varepsilon}_v^{acc}$. It also seems to temporarily increase the intensity of accumulation. For a respective modification of the HCA model further investigations are necessary.

ACKNOWLEDGEMENT

The study presented in the paper has been performed in the framework of the project A8 "Influence of fabric changes in soil on the lifetime of structures" of the collaborate research centre SFB 398 "Lifetime oriented design concepts" during the former work of the authors at Ruhr-University Bochum, Germany. The authors are grateful to DFG (German Research Council) for the financial support.

References

- [1] T. Doanh, Z. Finge, S. Boucq, and Ph. Dubujet. Histotropy of Hostun RF loose sand. In W. Wu and H.-S. Yu, editors, *Modern Trends in Geomechanics*, volume 106, pages 399–411. Springer, 2006.
- [2] K. Ishihara and H. Nagase. Multi-directional irregular loading tests on sand. *Soil Dynamics and Earthquake Engineering*, 7:201–212, 1988.
- [3] K. Ishihara and H. Takatsu. Effects of overconsolidation and K_0 conditions on the liquefaction characteristics of sands. *Soils and Foundations*, 19(4):59–68, 1979.
- [4] K. Ishihara and S. Yasuda. Sand liquefaction due to irregular excitation. *Soils and Foundations*, 12(4):65–77, 1972.
- [5] K. Ishihara and S. Yasuda. Sand liquefaction in hollow cylinder torsion under irregular excitation. *Soils and Foundations*, 15(1):29–45, 1975.
- [6] W.S. Kaggwa, J.R. Booker, and J.P. Carter. Residual strains in calcareous sand due to irregular cyclic loading. *Journal of Geotechnical Engineering, ASCE*, 117(2):201–218, 1991.

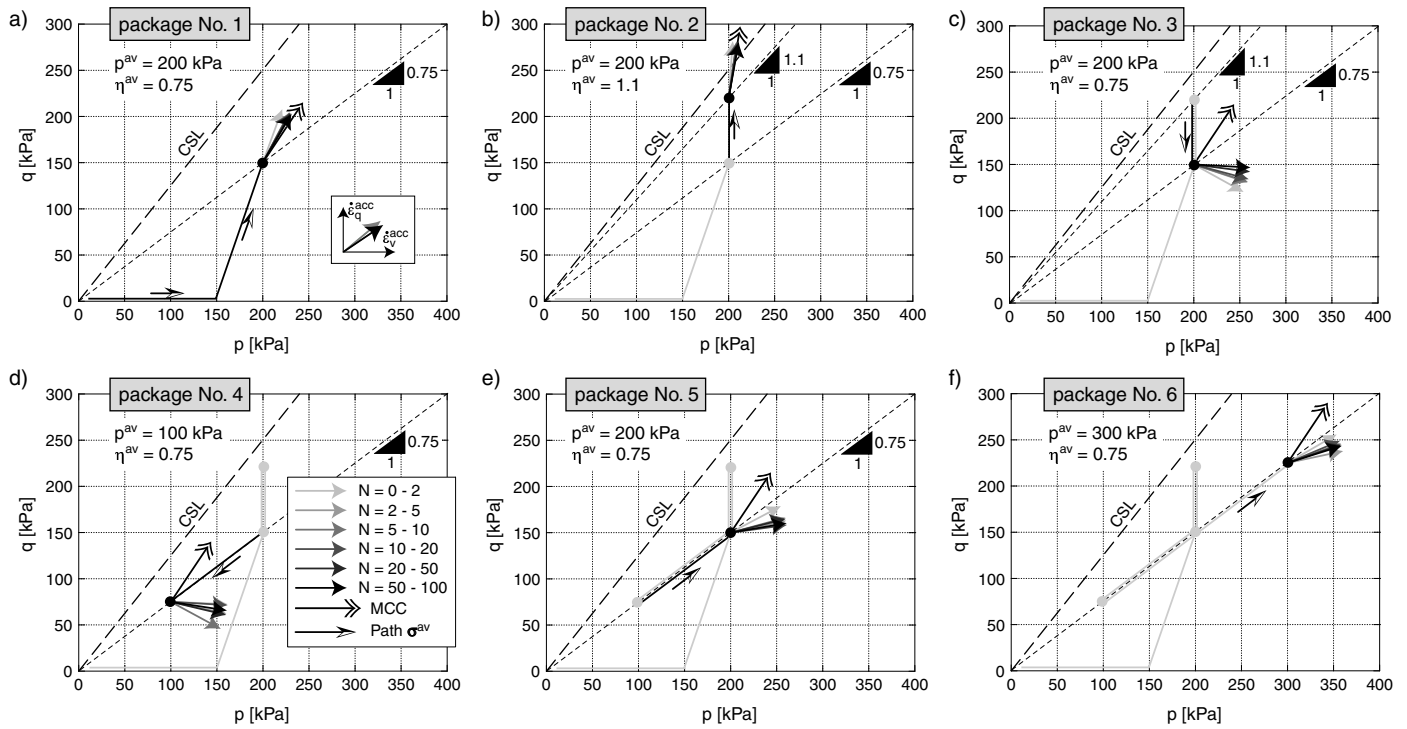


Fig. 14: Cyclic flow rule in tests with a change of the average stress σ^{av} between packages of cycles. The vectors start at σ^{av} and have an inclination of $\hat{\varepsilon}_q^{acc}/\hat{\varepsilon}_v^{acc}$ towards the horizontal.

- [7] M. Miner. Cumulative damage in fatigue. *Transactions of the American Society of Mechanical Engineering*, 67:A159–A164, 1945.
- [8] A. Niemunis, T. Wichtmann, and T. Triantafyllidis. A high-cycle accumulation model for sand. *Computers and Geotechnics*, 32(4):245–263, 2005.
- [9] H.B. Seed and I.M. Idriss. Simplified procedure for evaluating soil liquefaction potential. *Journal of the Soil Mechanics and Foundations Division, ASCE*, 97(SM9):1249–1273, 1971.
- [10] H.B. Seed, I.M. Idriss, F. Makdisi, and N. Banerjee. Representation of irregular stress time histories by equivalent uniform stress series in liquefaction analyses. Technical Report EERC 75-29, Univ. of California, Berkeley, Calif, 1975.
- [11] H.B. Seed and W.H. Peacock. Test procedures for measuring soil liquefaction characteristics. *Journal of the Soil Mechanics and Foundations Division, ASCE*, 97(SM8):1099–1119, 1971.
- [12] M.J. Shenton. Deformation of Railway Ballast under repeated loading conditions. *Railroad track mechanics and technology*. Pergamon Press, pages 405–425, 1978.
- [13] F. Tatsuoka, S. Maeda, K. Ochi, and S. Fujii. Prediction of cyclic undrained strength of sand subjected to irregular loadings. *Soils and Foundations*, 26(2):73–89, 1986.
- [14] T. Wichtmann, A. Niemunis, and T. Triantafyllidis. Strain accumulation in sand due to cyclic loading: drained triaxial tests. *Soil Dynamics and Earthquake Engineering*, 25(12):967–979, 2005.
- [15] T. Wichtmann, A. Niemunis, and T. Triantafyllidis. On the influence of the polarization and the shape of the strain loop on strain accumulation in sand under high-cyclic loading. *Soil Dynamics and Earthquake Engineering*, 27(1):14–28, 2007.
- [16] T. Wichtmann, A. Niemunis, and T. Triantafyllidis. Strain accumulation in sand due to cyclic loading: drained cyclic tests with triaxial extension. *Soil Dynamics and Earthquake Engineering*, 27(1):42–48, 2007.
- [17] T. Wichtmann, A. Niemunis, and T. Triantafyllidis. Validation and calibration of a high-cycle accumulation model based on cyclic triaxial tests on eight sands. *Soils and Foundations*, 49(5):711–728, 2009.
- [18] T. Wichtmann, A. Niemunis, and Th. Triantafyllidis. Simplified calibration procedure for a high-cycle accumulation model based on cyclic triaxial tests on 22 sands. In *International Symposium: Frontiers in Offshore Geotechnics, Perth, Australia*, 2010.
- [19] T. Wichtmann, H.A. Rondón, A. Niemunis, T. Triantafyllidis, and A. Lizcano. Prediction of permanent deformations in pavements using a high-cycle accumulation model. *Journal of Geotechnical and Geoenvironmental Engineering, ASCE*, 136(5):728–740, 2010.
- [20] T.L. Youd. Compaction of sands by repeated shear straining. *Journal of the Soil Mechanics and Foundations Division, ASCE*, 98(SM7):709–725, 1972.